

A New Thermodynamic Description of the Cu-Zr System

K.-J. Zeng and M. Härmäläinen*
Laboratory of Materials Processing and Powder Metallurgy
Helsinki University of Technology
Vuorimiehentie 2K, SF-02150, Espoo, Finland
 and
H.L. Lukas
Max-Planck Institut für Metallforschung
Institut für Werkstoffwissenschaft
Heisenbergstr. 5, D-7000 Stuttgart 80, Germany

(Submitted July 15, 1994; in revised form September 7, 1994)

An optimized set of thermodynamic functions for the Cu-Zr system was obtained by the least squares method from phase diagram and thermodynamic data available in the literature. The excess Gibbs energies of the solution phases, liquid, and three terminal solid solutions, were described by the Redlich-Kister formula. All the intermediate compounds were treated as stoichiometric phases. The calculated phase diagram, as well as the thermodynamic properties vs compositions, agree well with the experimental values. The reliability of the optimized parameters was examined using μ - T plots.

1. Introduction

Copper and its alloys are used extensively in electrical and electronic applications where conductivity, strength, and formability are required. Examples include electric connectors, thermal conduction plates, and welding electrode tips. Several alloys are available that utilize precipitation or dispersion hardening, but the accompanying electrical conductivity is low. As a further limitation, these alloys usually contain expensive and/or hazardous elements, such as silver, cadmium, and beryllium, in order to produce an acceptable level of properties. It has been found that using zirconium as the primary alloying element in the copper alloys can achieve useful combinations of strength and electrical conductivity.^{1,2,3,4} Knowledge of the phase relations in the copper-base alloys containing zirconium and their thermodynamic behavior is essential for improving the properties of these alloys and optimizing the production techniques.

The Cu-Zr phase diagram is characterized by several intermetallic compounds. However, there is much confusion regarding

the compositions of these phases in the literature, particularly the Cu-rich ones. This confusion is also reflected by the previous calculations of the system.^{5,6} Since the accuracy of the thermodynamic description of a binary system is crucial for the prediction of ternary and higher order phase diagrams, a new thermodynamic description of the Cu-Zr system is developed here.

2. Previous Calculations

The Cu-Zr system has been thermodynamically analyzed three times.^{5,6,7} In order to quantitatively predict the glass formation range of the Cu-Zr system, Saunders⁵ calculated the Cu-Zr phase diagram based on the old version of compilations of the system by Hansen,⁸ Elliott,⁹ and Shunk¹⁰ and the thermodynamic studies by Kleppa and Watanabe¹¹ and Ansara et al.¹² Unfortunately, the Cu-richest compound phase Cu₅Zr, which

*Present address: Technische Universität Clausthal, AG Elektronische Materialien, Robert-Koch-Str. 42, D-38678, Clausthal-Zellerfeld, Germany.

Table 1 Comparison between the Measured and the Calculated Enthalpies of Formation of the Compounds in the Cu-Zr System

Compound	Ref. 5	Calculated enthalpies, J/mol		This work	Measured enthalpies, J/mol	
		Ref. 6			Ref. 11	Ref. 12
Cu ₅ Zr.....	...	-2 207.24		-10 299 00	..	.
Cu ₅₁ Zr ₁₄	-11 230	-2 905.94		-12 975.58	-14 070	...
Cu ₈ Zr ₃	-15 816	-3 245.93		-13 460.29
Cu ₁₀ Zr ₇	-21 226	-6 735.12		-14 220.59	-12 310	...
CuZr.....	-24 012	-7 337.17		-10 052.12	-9 050	-24 400
CuZr ₂	-17 167	-12 726.92		-14 634 67	-10 950	-17 300

Note: Mol is mole of atoms. Some stoichiometries used in the cited references are different from those listed here.

Section I: Basic and Applied Research

is an important strengthening phase in Cu-Zr based electrical and electronic materials, was not included. The stoichiometries used for the five compound phases included are Cu_4Zr , Cu_5Zr_2 , $\text{Cu}_{10}\text{Zr}_7$, CuZr , and CuZr_2 . The general features of the then-accepted phase diagram were reproduced, except for the compound $\text{Cu}_{10}\text{Zr}_7$, which was predicted to be formed peritectically. The calculated liquidus of Cu_4Zr is more rich in copper than the measured one. The optimized enthalpies of formation of the congruent melting compounds differ largely from the experimental data reported by Kleppa et al.,¹¹ but those of CuZr and CuZr_2 are very close to the values of Ansara et al.¹² (see Table 1).

Using the phase equilibrium information in the published phase diagram¹³ combined with the experimental results of Kneller et al.¹⁴ and the thermodynamic data measured by Kleppa et al.,¹¹ Bormann et al.⁷ calculated the free energies of the metastable amorphous phase and equilibrium solution phases in the Cu-Zr system. The curves of Gibbs energies of these phases have been presented, but the thermodynamic parameters have not been reported.

Since the calculation by Saunders,⁵ more reasonable phase stabilities of elements have been published,¹⁵ and new experimental results have become available on the phase diagram in copper-rich region¹⁶ and the thermodynamic properties of liquid alloys.^{17,18} Luoma and Talja⁶ recalculated the system incorporating more experimental data¹⁶⁻¹⁹ but using the same models as Saunders.⁵ The phase diagram evaluated by Lou and Grant²⁰ was used as the basis. The stoichiometries of the compounds were taken as Cu_5Zr , $\text{Cu}_{36}\text{Zr}_{10}$, $\text{Cu}_{72}\text{Zr}_{28}$, $\text{Cu}_{10}\text{Zr}_7$, CuZr , and CuZr_2 . Although the calculated phase diagram agrees excellently with the experimental data, and a good fit has been obtained to the measured thermodynamic properties of the liquid phase, the assessment is open to two concerns: (a) the assessed enthalpies of formation of the four Cu-rich compounds are too small (see Table 1), and (b) the μ - T diagrams calculated by using their parameters show that all the compound phases, except for CuZr_2 , tend to decompose at room temperature.

3. Experimental Information

The extensive literature survey for the Cu-Zr system by Arias and Abriata²¹ was utilized as the basis in the present work. The most recent information was scanned from the database THERMET at LTPCM in Grenoble, France.

3.1 Stoichiometries of the Intermetallic Compounds

It is generally accepted that there are six intermediate compounds in the Cu-Zr system.^{13,16,20,21,22} Arias and Abriata²¹ assessed the stoichiometries of these compounds as Cu_9Zr_2 , $\text{Cu}_{51}\text{Zr}_{14}$, Cu_8Zr_3 , $\text{Cu}_{10}\text{Zr}_7$, CuZr , and CuZr_2 . Kneller et al.¹⁴ reported four extra phases: Cu_2Zr , $\text{Cu}_{24}\text{Zr}_{13}$, $\text{CuZr}_{1+\nu}$, and Cu_5Zr_8 , but Arias and Abriata²¹ supposed that the experimental procedure followed by Kneller et al.¹⁴ is open to several questions. In accord with their opinion, these four compounds were omitted from the present work. For the detailed discussion about this point, readers are referred to Arias and Abriata.²¹

Table 2 Experimental Methods Employed in the Study of the Cu_5Zr Phase

Reference	Sample	Method
20.....	Extracted precipitate	XRD
34.....	Diffusion couple	Metallography, microhardness, EPMA
35.....	Diffusion couple	Metallography, microhardness, EPMA
36.....	As-cast alloy	Metallography, EPMA
37.....	Aged alloy	Electron microscopy
38.....	Aged Cu_5Zr alloy	XRD
39.....	Aged alloy	EDS
40.....	Spray-cast alloy	Electron diffraction

The formulas of the compounds used in the present work are Cu_5Zr , $\text{Cu}_{51}\text{Zr}_{14}$, Cu_8Zr_3 , $\text{Cu}_{10}\text{Zr}_7$, CuZr , and CuZr_2 , of which the Cu_5Zr is different from the assessed Cu_9Zr_2 by Arias and Abriata,²¹ and the first three are different from those employed by Luoma and Talja.⁶ Therefore, it is necessary to give a review on the stoichiometries of these three phases.

3.1.1 Cu_5Zr . Because of its importance in strengthening the electronic conductor of copper alloys, the most copper-rich compound in the Cu-Zr system was subjected to many investigations. A number of structure-property relationship studies on Cu-Zr and Cu-Cr-Zr alloys identified Cu_3Zr as the Zr-containing precipitate phase.^{2,23-26} This is in agreement with the results of some other investigations.²⁷⁻³¹ On the basis of electron probe microanalysis of as-cast alloys near the composition of Cu_4Zr , Donachie³² stated that the first phase was Cu_4Zr . Using the empirical method of Ziebold and Ogilvie, Vitek²² evaluated the compositions of the intermediate phases in the Cu-Zr system and suggested that the first compound has a composition between Cu_9Zr_2 and Cu_4Zr , slightly favoring the Cu_9Zr_2 composition. Afterwards, the analysis results of metallography, X-ray, and electron probe microanalysis (EPMA) by Glimois et al.,¹⁶ Kuznetsov et al.,¹⁹ and Forey et al.³³ established the stoichiometry of this compound as Cu_9Zr_2 . However, Glimois et al.¹⁶ also determined that the room temperature crystal structure of this phase is a tetragonal long-period superlattice derived from the AuBe_5 -type structure, and more investigations determined this compound as Cu_5Zr .^{20,34-40} The experimental methods used in these investigations are listed in Table 2.

Because the Zr weight percentages of the first compound obtained by different electron probe microanalysis show a large scatter (28.1,³² 25.0,²² 25,³⁴ unknown,³⁵ 21.7³⁶), Lou and Grant²⁰ assumed that electron probe microanalysis is not well suited for resolving detailed compositional differences. Instead of EPMA, they used electrolytic extraction to isolate the Cu-Zr precipitate phase from the matrices of aged copper alloys with a dilute addition of Zr, and used X-ray diffraction (XRD) to analyze the extracted phase. Their diffraction pattern clearly matches those calculated and observed for polycrystalline Cu_5Zr by Forey et al.³⁸ Recently, by using selected area diffraction (SAD) and energy dispersive X-ray analysis, Singh et al.^{40,55} confirmed the presence of the Cu_5Zr phase in the Cu-Zr alloys in the composition range of 0.1 to 0.8 wt.% Zr, and concluded that the first compound phase of the Cu-Zr system is

Cu₅Zr. Therefore, the formula Cu₅Zr was accepted in the present work.

3.1.2 Cu₅Zr₁₄. Various stoichiometries for the second compound of the Cu-Zr system have been suggested in the literature. It was identified as Cu₄Zr by means of electron probe microanalysis.^{32,34,35,36} On the basis of experimental results of metallography, X-ray, and thermal analysis, Lundin et al.³⁰ supported the existence of an intermediate compound close to Cu₃Zr, which was reported previously by Allibone and Sykes,²⁷ Pogodin et al.,²⁸ and Raub and Engel.²⁹ Vitek²² assumed that the second compound was Cu₃₆Zr₁₀, which was afterwards accepted by Lou and Grant.²⁰ Kuznetsov et al.¹⁹ used Cu₇Zr₂ to describe the phase with the highest congruent melting point in the Cu-Zr system. Gabathuler et al.⁴¹ determined by means of XRD the crystal structure of the isostructural phase in the Cu-Hf system and found it to possess the Ag₅₁Gd₁₄ type structure; hence the composition of the corresponding Cu-Zr phase was determined as Cu₅₁Zr₁₄. This composition was confirmed independently by Bsenko.⁴²

3.1.3 Cu₈Zr₃. Luoma and Talja⁶ used Cu₇Zr₂₈ for the third compound in this system. In the present work, however, the formula Cu₈Zr₃ was preferred. Lundin et al.³⁰ made the first observation of a peritectic phase at ~30 at.% Zr in the Cu-Zr system. The phase was then tentatively assigned the formula Cu₅Zr₂. Hillmann and Hofmann³⁴ and Meny et al.³⁵ proposed Cu₃Zr for this phase, but the evidence obtained by Perry and Hugi³⁶ and Phillips³⁷ indicates that Cu₅Zr₂ may be more correct. Kuznetsov et al.¹⁹ and Vitek²² supported this viewpoint. Later, Bsenko^{42,43} showed that this peritectic compound has an orthorhombic structure and is isostructural with Cu₈Hf₃. Bsenko⁴³ also stated that the formula Cu₈Zr₃ is in better agreement with the microprobe results of Vitek²² than Cu₅Zr₂. In the Cu-Zr phase diagram revised by Lou and Grant,²⁰ the formula Cu₇Zr₂₈ was used for this phase, but no experimental evidence was reported.

3.2 Phase Diagram Data

The liquidus investigations of the Cu-Zr system are summarized in Table 3. The liquidus appears to be reasonably well determined for the compositions between 10 and 30 at.% Zr. Although the work of Lundin et al.³⁰ covered the whole system, only a few points were determined on the liquidus. Glimois et al.¹⁶ and Kuznetsov et al.¹⁹ measured the liquidus curve by means of thermal analysis and metallography in the approximate composition range 10 to 30 at.% Zr. Their results are in good agreement with those of Lundin et al.³⁰ All the measured liquidus points by Pogodin et al.²⁸ agree quite well with the above-mentioned experimental results except one point, which was claimed as the melting point of Cu₃Zr. In the approximate composition range of 0 to 36 at.% Zr, there is general agreement among the data from Raub and Engel,²⁹ Pogodin et al.,²⁸ Lundin et al.,³⁰ Kuznetsov et al.,¹⁹ and Glimois et al.¹⁶ In the rest of the range, the measured liquidus by Raub and Engel²⁹ is located much higher than that by Lundin.³⁰ Therefore, the values of Raub and Engel²⁹ in this range were not used in the present optimization. The liquidus data of Auguston⁴⁴ on the Zr-rich side scatter widely and were not considered in the present work.

Because of its technological importance, the solubility of Zr in (Cu) has been examined many times (Table 4). Limited results obtained by Raub and Engel²⁹ indicated that zirconium solubility in copper is <0.091 at.% at 1213 K. On the basis of a metallographic examination of equilibrated copper-rich Cu-Zr alloys, Saarivirta²³ determined both (Cu) solidus and solvus and placed the maximum solubility of zirconium in copper at 0.105 at.% and 1253 K. By means of metallographic and electrical measurements, Zwicker²⁴ determined the (Cu) solvus. Analyzing metallographically the (Cu) alloys, which were cold worked, solution treated, and quenched, Kawakatsu et al.²⁵ determined the solubility of Zr in (Cu) at 1173 and 1223 K. These four experimental results^{23,24,25,29} are in very good agreement. The (Cu) solvus determined by Showak⁴⁵ using metallographic and electrical measurement agrees generally with the four results, but in the higher temperature region close to the eutectic temperature, his values are larger. Pogodin et al.²⁸ reported a much larger solubility of Zr in (Cu). Their data were discarded from the present work.

There is limited information on the solid solubility of Cu in (βZr) or (αZr). Lundin et al.³⁰ examined metallographically the phase boundaries of (βZr) and (αZr) using equilibrated alloys. Based on the measured volume fraction of CuZr₂ in the equilibrated alloys in (βZr) + CuZr₂ two-phase region, Douglass and Morgan⁴⁶ calculated the solubilities of Cu in (βZr) by applying an analytical treatment. The results agree generally with the metallographic observation by Lundin et al.³⁰

Table 3 Summary of Cu-Zr Liquidus Investigations

Reference	Experimental method	Approximate composition range
16	Thermal analysis, metallography	14 to 22
19	Thermal analysis, metallography, EPMA	10 to 30
28	Thermal analysis, metallography	0 to 27
29	Thermal analysis	0 to 60
30	Thermal analysis, metallography	0 to 100
44	Thermal analysis, metallography	40 to 100

Table 4 Summary of Solid Solubility Investigations

Reference	Experimental method	Solid solution phase
23	Metallography	(Cu)
24	Metallography, electrical resistivity	(Cu)
25	Metallography	(Cu)
28	Thermal analysis, metallography	(Cu)
29	Thermal analysis, metallography	(Cu)
30	Metallography	(βZr), (αZr)
45	Metallography, electrical resistivity	(Cu)
46	Quantitative metallography	(βZr)
47	Microhardness, electrical resistivity	(Cu)

Section I: Basic and Applied Research

Table 5 Comparison between the Measured, Assessed, and Calculated Temperatures of the Three-Phase Equilibria in the Cu-Zr System and the Compositions of the First Phase in the Equilibrium Reaction Formulas

Equilibrium	Method	Temperature, K	Composition of the first phase, at. % Zr	Reference		
L ↔ (Cu) + Cu ₅ Zr	Measured	1253	9.35	28		
		1250	9.95	29		
		1237	9.1	27		
		1238	6.5	30		
		1253	...	23		
		1253	...	45		
		~1243	9.8	32		
		1244	8.9	36		
		1240	~8.2	19		
		1250	~8.8	16		
		Assessed	1245	8.6	21	
		Calculated	1241	7.69	This work	
		L + Cu ₅₁ Zr ₁₄ ↔ Cu ₅ Zr	Measured	1283	~10.7	19
				1287	...	16
				Assessed	1285	~11.5
Calculated	1288			10.7	This work	
L + Cu ₅₁ Zr ₁₄ ↔ Cu ₈ Zr ₃	Measured	1343	30.81	30		
		1248	...	19		
		Assessed	1248	~36	21	
		Calculated	1195	38.8	This work	
L ↔ Cu ₈ Zr ₃ + Cu ₁₀ Zr ₇	Measured	1158	38.2	30		
		Assessed	1158	~38.2	21	
		Calculated	1164	40.8	This work	
L ↔ Cu ₁₀ Zr ₇ + CuZr	Measured	1163	44	30		
		Assessed	1163	~44	21	
		Calculated	1163	42.5	This work	
L ↔ CuZr + CuZr ₂	Measured	1201	54.3	30		
		Assessed	1201	~54.3	21	
		Calculated	1197	53.8	This work	
L ↔ CuZr ₂ + (βZr)	Measured	1271	73.95	44		
		1268	72.4	30		
		Assessed	1268	~72.4	21	
		Calculated	1270	70.0	This work	
		(βZr) ↔ CuZr ₂ + (αZr)	Measured	1189	93	44
1095	97.8			30		
Assessed	1095			97.8	21	
Calculated	1089			97.6	This work	
CuZr ↔ Cu ₁₀ Zr ₇ + CuZr ₂	Measured	988	50	48		
		Assessed	988	50	21	
		Calculated	977	50	This work	

The experimental data for the three-phase equilibria and the melting points of congruent compounds are listed in Tables 5 and 6, respectively. The investigations were concentrated on the Cu-rich side. The equilibrium temperature of $L \leftrightarrow (Cu) + Cu_5Zr$ as well as the melting point of $Cu_{51}Zr_{14}$ have been well determined.

The experimental work of Auguston⁴⁴ probably had a serious oxygen contamination problem because his reported eutectoid temperature (1189 K) of $(\beta Zr) \leftrightarrow CuZr_2 + (\alpha Zr)$ is even much higher than the transformation temperature of $(\alpha Zr) \leftrightarrow (\beta Zr)$. These data were not incorporated in the optimization.

The high-temperature magnetic susceptibility measurements and the metallographic studies carried out by Carvalho and Harris⁴⁸ indicate that the compound phase $CuZr$ decomposes eutectoidally at 988 ± 5 K. The Cu-50 at. % Zr alloy annealed at 900 K for 24 h and then furnace-cooled to room temperature shows a typical eutectoid structure with alternative areas of the component phases. Because this is the only data concerning

the reaction $CuZr \rightarrow Cu_{10}Zr_7 + CuZr_2$, it was used in optimization with a small weight factor.

There is a great difference between the equilibrium temperatures of $L + Cu_{51}Zr_{14} \leftrightarrow Cu_8Zr_3$ measured by Lundin et al.³⁰ and Kuznetsov et al.¹⁹ The data of Kuznetsov et al.¹⁹ were used in optimization but were given a small weight. The three-phase equilibrium $Cu_8Zr_3 \leftrightarrow Cu_{51}Zr_{14} + Cu_{10}Zr_7$ at $885^\circ K$ observed by Kneller et al.¹⁴ was not used because of the experimental problems mentioned in section 3.1.

3.3 Thermodynamic Data

The enthalpy of mixing of liquid Cu-Zr alloys has been studied by three groups of investigators^{11,17,18} by means of high-temperature reaction calorimetry at 1373, 1480, and 1473 K, respectively. There is very good agreement among these data. Sommer and Choi¹⁸ also measured the copper activities in liquid Cu-Zr alloys at 1499 K on the basis of the Knudsen effusion method using collector technique.

Table 6 Comparison between the Measured, Assessed, and Calculated Congruent Melting Points of Intermetallic Compounds in the Cu-Zr System

Phase	Method	Temperature, K	Reference
Cu ₅ Zr ₁₄	Measured	1373	30
		1386	36
		1388	16
		1413	28
		1385	29
	Assessed Calculated	1377	19
		1388	21
		1395	5
		1386	This work
		1208	30
CuZr.....	Measured	1208	30
	Assessed	1208	21
	Calculated	1201	5
CuZr ₂	Measured	1209	This work
		1338	44
		1273	30
	Assessed	1273	21
		1284	5
Cu ₁₀ Zr ₇	Measured	1275	This work
		1168	30
		1168	21
	Assessed	1189(a)	5
		1164.4	This work

(a) Peritectic temperature.

Kleppa and Watanabe¹¹ measured the enthalpies of formation of the four congruent melting compounds in the Cu-Zr system by drop calorimetry or by solution calorimetry in liquid copper. Although discrepancies exist between the analytical and prepared compositions of the alloy samples, their data can be used in the optimization because small deviations from stoichiometry should have little influence on the observed heat content. Independently, Ansara et al.¹² determined the enthalpies of formation of CuZr and CuZr₂ by means of solution calorimetry in liquid aluminum. A significant discrepancy exists between these two investigations. Because the compound CuZr decomposes eutectoidly at 988 K,⁴⁸ its enthalpy data must be much smaller than that of a mixture of the produced phases Cu₁₀Zr₇ and CuZr₂. The data by Ansara et al.¹² do not satisfy this requirement and, therefore, were not used in the optimization.

4. Thermodynamic Modeling

4.1 Unary Data

The Gibbs energies of the pure elements vs temperature $G^0(T) = G(T) - H^{SER}$ (298.15 K) were represented by Eq 1:

$$G^0(T) = a + bT + cT \ln(T) + dT^2 + eT^{-1} + fT^3 + iT^4 + jT^7 + kT^{-9} \quad (\text{Eq 1})$$

H^{SER} is the enthalpy of the "Stable Element Reference," the pure element in its stable state at 298.15 K and 10⁵ Pa, for example, fcc Cu and cph Zr. The temperature may be divided into several ranges, where the coefficients $a, b, c, d, e, f, i, j,$ and k have different values. The values of these coefficients were taken from Dinsdale.¹⁵

4.2 Solution Phases

For the concentration dependence of G of the liquid phase and the three terminal solid solutions, the Redlich-Kister formula⁴⁹ was used:

$$G - H^{SER} = \sum_{i=1}^2 x_i G_i^0 + RT \sum_{i=1}^2 x_i \ln(x_i) + G^{ex} \quad (\text{Eq 2})$$

$$G^{ex} = x_1 x_2 \sum_{n=0}^m (x_1 - x_2)^n L_n \quad (\text{Eq 3})$$

$$L_n = a_n + b_n T + c_n T \ln(T) \quad (\text{Eq 4})$$

where L_n are the interaction parameters, a_n describes the enthalpy of mixing, b_n is the excess entropy of mixing, and c_n is the heat capacity of mixing.

4.3 Intermetallic Compound Phases

Because no experimental data were available on the homogeneity ranges of the Cu-Zr compound phases, all the compounds were treated as stoichiometric phases. The Gibbs energies of formation of these phases were written as $\Delta_f G$ parameters:

$$\Delta_f G_{Cu_p Zr_q} = G_{Cu_p Zr_q} - pG_{Cu}^{0, fcc} - qG_{Zr}^{0, cph} = a + bT \quad (\text{Eq 5})$$

where $G_{Cu_p Zr_q}$ is the Gibbs energy of the compound phase Cu_pZr_q.

5. Optimization Procedure

5.1 Selection of the Adjustable Coefficients

Because every parameter to be optimized in the thermodynamic model of a phase has its own physicochemical meaning, the quality of optimization of thermodynamic parameters and calculation of phase diagram depend strongly on the selection of adjustable parameters. This makes the thermodynamic optimization quite different from the pure mathematical one where one can add more adjustable parameters one by one until the measured curve can be reproduced. In the thermodynamic optimization of phase diagrams, however, one should consider what thermodynamic quantities are connected with the measured values and how these quantities are connected with the parameters. From these considerations, one can get the best ideas how many and which of the parameters can be adjusted. Only those parameters that are determined by the experimental values are adjusted. With an inefficient set of parameters, the description may be unable to reproduce experimentally well-established features of the thermodynamic properties. On the other hand, too many parameters may reduce the optimization to an arbitrary mathematical smoothing. The calculation of phase diagram by using these parameters may lead to strange results in the areas that are not covered by experimental values.

As reviewed in section 3.3, the enthalpies of mixing of the liquid Cu-Zr alloys have been measured, and the experimental data on the liquidus curve are available in a large temperature range. Therefore, the temperature dependence of excess Gibbs energy, b_n in Eq 4, of the liquid phase can be adjusted inde-

Section I: Basic and Applied Research

pendently. The experimental results^{11,17,18} show that the effect of temperature on the enthalpies of mixing of the liquid alloys can be neglected. Hence, the coefficients c_n were not optimized and taken to be zero. After several attempts using different numbers of parameters, the subregular model (with $m = 1$ in Eq 3) was chosen for the liquid phase.

Because the solubilities of the Cu-Zr solid solutions are rather limited, the composition dependence of interaction between elements in these phases can be neglected. So only the coefficient a_0 in Eq 4 was used for the terminal solution phases (Cu), (β Zr), and (α Zr).

The temperature dependence of Gibbs energy of formation or the coefficient b in Eq 5 for the congruent melting compounds CuZr and CuZr₂ can be optimized independently because their enthalpies of formation have been experimentally determined, and their Gibbs energies are well known at two different temperatures, the congruent melting temperature and the eutectoid decomposition temperature. However, it is not the case for Cu₅Zr. Although its Gibbs energy is known at two different temperatures, the equilibrium temperatures of L \leftrightarrow (Cu) + Cu₅Zr and L + Cu₅Zr₁₄ \leftrightarrow Cu₅Zr, the temperature difference is too small to adjust its enthalpy and entropy of formation independently. Similarly, the coefficient b of Cu₈Zr₃ in Eq 5 also cannot be adjusted independently because its peritectic formation temperature has not been well determined.

The situation of Cu₅₁Zr₁₄ and Cu₁₀Zr₇ is more complicated. Even though their enthalpies of formation have been experimentally determined and their Gibbs energies are known at two different temperatures, the congruent melting temperature and the three-phase equilibrium temperature, it was found during suboptimizations that when the coefficients b in Eq 5 were introduced for them, their coefficients a became much smaller than the experimentally determined enthalpies of formation, and the coefficients b were negative. Furthermore, the values of a and b of these two compounds were very sensitive to the weight factors designated to the phase diagram data on the Zr-rich side and changed largely in different suboptimizations. These phenomena indicated that the temperature dependence of Gibbs energy of formation of Cu₅₁Zr₁₄ and Cu₁₀Zr₇ could not be optimized independently. Therefore, the coefficients b of the compounds Cu₅₁Zr₁₄ and Cu₁₀Zr₇, together with Cu₅Zr and Cu₈Zr₃, were assumed to be zero.

5.2 Input of Enthalpy Data of Liquid Phase

In the calorimetric measurement, usually small amounts of the second element M_2 (Δn_{M_2}) are successively added to the calorimetric bath, which contains liquid M_1 - M_2 alloys or at the beginning of the pure element M_1 , and the heat effects associated with each addition ($\Delta_{\text{obs}}H$) are measured. From the measured heat effects $\Delta_{\text{obs}}H$, the integral enthalpies of mixing of liquid M_1 with solid M_2 ($\Delta_{\text{mix}}H^{L-s}$) or liquid M_1 with liquid M_2 ($\Delta_{\text{mix}}H^{L-L}$) can be calculated as follows:

$$\Delta_{\text{mix}}H^{L-s}(T) = (\sum \Delta_{\text{obs}}H - \sum \Delta n_{M_2} H_{M_2}) / \sum n_i \quad (\text{Eq 6})$$

$$\Delta_{\text{mix}}H^{L-L}(T) = \Delta_{\text{mix}}H^{L-s}(T) - x_{M_2} \Delta_{\text{fus}}H_{M_2} \quad (\text{Eq 7})$$

where H_{M_2} is the heat content of element M_2 from room temperature to the experimental one T , $\Delta_{\text{fus}}H_{M_2}$ is the enthalpy of metastable melting of M_2 at experimental temperature T , and n_i is the amount of element i in the calorimetric bath.

The values of $\Delta_{\text{mix}}H^{L-L}$ and $\Delta_{\text{mix}}H^{L-s}$ calculated this way could not be used in the least squares optimization because their statistical errors do not have Gaussian normal distribution, which is a requirement of the least squares method. A detailed discussion on this point was given by Lukas and Fries.⁵⁰ In the present work, the heat effect of mixing for each addition of zirconium ($\Delta_{\text{obs}}H$) were calculated from the reported values of $\Delta_{\text{mix}}H^{L-s}$ by Kleppa et al.¹¹ and Sommer et al.,¹⁸ values of $\Delta_{\text{mix}}H^{L-L}$ by Sudavtsova et al.,¹⁷ and input into the data file for optimization.

5.3 Optimization

The optimization and calculation programs developed by Lukas et al.⁵¹ were used for the present calculation of the Cu-Zr system. Since the experimental data from different sources are often not consistent and even cannot be reconciled with each other in some cases, the optimization procedure strongly depends on how much one attempts to fit experimental data. On the other hand, the parameters obtained here are expected to be used in the Cu-Cr-Zr ternary system. Therefore, each piece of experimental information was analyzed and then given a certain weight in optimization in order to get the most acceptable compromise between the scattered experimental data. The approach to do this is to carry out separate suboptimizations for one or two phases using various selections of the available experimental data.

The computerized optimization of the Cu-Zr system started with optimizing only the liquid phase to the thermodynamic data available. The copper activity and the enthalpy of mixing were readily described using the chosen model and adjustable coefficients. Then the phases Cu₅₁Zr₁₄, Cu₅Zr, and (Cu) were added one by one successively to fit the phase diagram data and thermodynamic properties simultaneously.

In the next step, the parameters of these phases were kept constant because they have been well determined from the available experimental data. The other phases in equilibrium with liquid were added one by one, from the left to the right side of the Cu-Zr phase diagram. Then using the obtained values of parameters of these phases as start values, all the solid phases in the approximate composition range 40 to 100 at.% Zr were optimized together to fit the invariant equilibrium data.

Finally, the whole system was optimized using the selected experimental data and the weight factors determined in the previous suboptimizations. The parameters already obtained were changed a little in this step.

6. Results and Discussion

The thermodynamic parameters resulting from this least squares procedure are given in Table 7. The phase diagram calculated with these parameters is shown in Fig. 1 and compared in Fig. 2 to 4 with the experimental data from literature. The predicted invariant equilibria are compared in Tables 5 and 6

Table 7 Optimized Thermodynamic Parameters for the Cu-Zr System

Redlich-Kister⁴⁹ formalism for the solution phases (Eq 2 to 4)

liquid.....
 (Cu).....
 (βZr).....
 (αZr).....

$$L_0 = 61\,685.53 + 11.29235 T$$

$$L_1 = -8830.66 + 5.04565 T$$

$$L_0 = +2233$$

$$L_0 = -7381.13$$

$$L_0 = +11\,336.85$$

Gibbs energies of formation of the compound phases (Reference states: fcc Cu and cph Zr)

Cu₅Zr.....
 Cu₅₁Zr₁₄.....
 Cu₈Zr₃.....
 Cu₁₀Zr₇.....
 CuZr.....
 CuZr₂.....

$$\Delta_f G = -10\,299.00$$

$$\Delta_f G = -12\,975.58$$

$$\Delta_f G = -13\,460.29$$

$$\Delta_f G = -14\,220.59$$

$$\Delta_f G = -10\,052.12 - 3.81598 T$$

$$\Delta_f G = -14\,634.67 + 1.73017 T$$

Note: Values are in J/mol and J/K · mol where mol is mole of atoms.

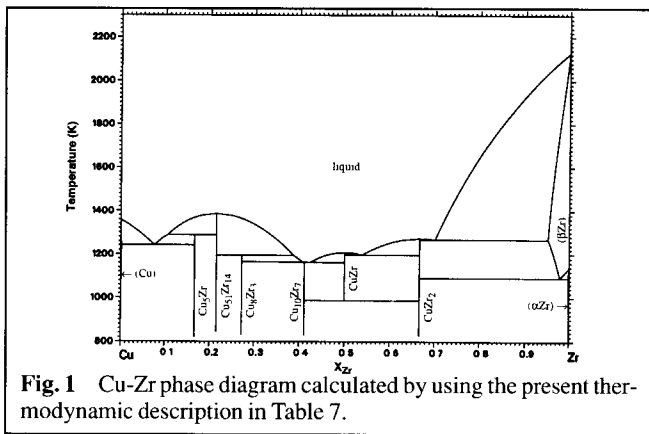


Fig. 1 Cu-Zr phase diagram calculated by using the present thermodynamic description in Table 7.

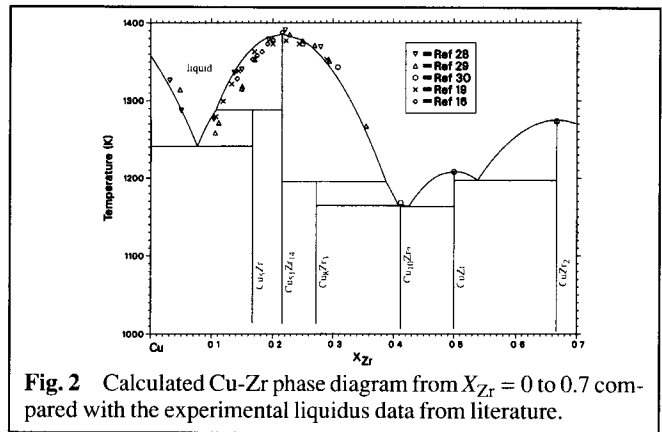


Fig. 2 Calculated Cu-Zr phase diagram from $X_{Zr} = 0$ to 0.7 compared with the experimental liquidus data from literature.

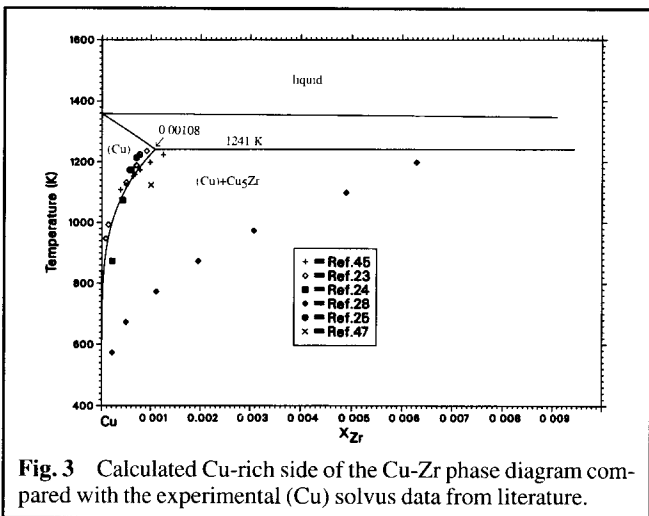


Fig. 3 Calculated Cu-rich side of the Cu-Zr phase diagram compared with the experimental (Cu) solvus data from literature.

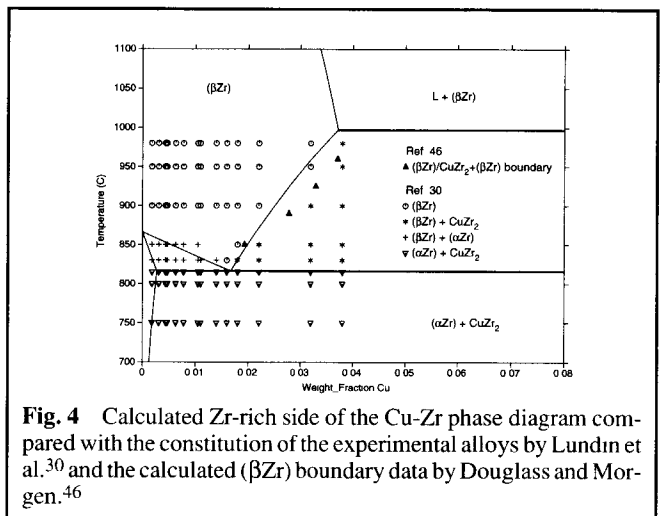


Fig. 4 Calculated Zr-rich side of the Cu-Zr phase diagram compared with the constitution of the experimental alloys by Lundin et al.³⁰ and the calculated (βZr) boundary data by Douglass and Morgen.⁴⁶

with the experimental data from different sources, the assessed values by Arias and Abriata,²¹ and the calculation results by Saunders.⁵

A very good fit to the measured liquidus data was obtained (Fig. 2). The calculated solvus of (Cu) agrees very well with the experimental results, especially the solvus by Saarivirta²³ (Fig. 3). The calculated maximum solubility of Zr in (Cu) is

0.108 at.%, which is close to the assessed value, ~0.12 at.%, by Arias et al.²¹

In Fig. 4, the calculated phase diagram is compared with the constitution of experimental alloys on the Zr-rich side analyzed by Lundin et al.³⁰ using X-ray and metallographic techniques and the analytically calculated (βZr) boundary data by Douglass and Morgen.⁴⁶ The thermodynamic description ob-

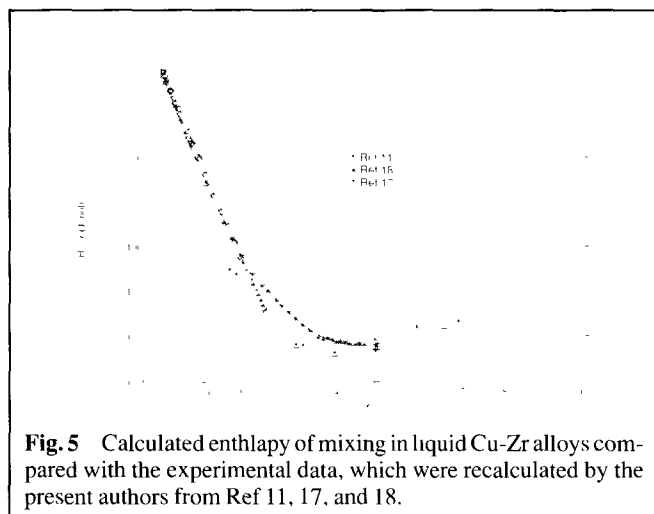


Fig. 5 Calculated enthalpy of mixing in liquid Cu-Zr alloys compared with the experimental data, which were recalculated by the present authors from Ref 11, 17, and 18.

tained here accounts very well for almost all of the experimental observations. The calculated maximum solubility of Cu in (β Zr) and (α Zr), 5.26 and 0.39 at.%, respectively, can be regarded as a satisfactory representation of the observed diagram. The predicted (β Zr)/(β Zr) + CuZr₂ boundary is also in good agreement with the analytical calculation by Douglass and Morgan.⁴⁶

From Fig. 2 to 4 and Tables 5 and 6, it can be seen that the calculated Cu-Zr phase diagram agrees well with the experimental information except for the three-phase equilibrium $L \leftrightarrow \text{Cu}_8\text{Zr}_3 + \text{Cu}_{10}\text{Zr}_7$, of which the eutectic composition was calculated to be 40.8 at.% Zr, very close to the composition of Cu₁₀Zr₇. In addition, the difference between the calculated eutectic temperature and the congruent melting point of Cu₁₀Zr₇ are too small (Fig. 2). Cu₁₀Zr₇ was even calculated to be formed peritectically by Saunders.⁵ Because this phase is in the center of glass forming range,⁵² and the experimental results of Lundin et al.³⁰ involving this phase have not been confirmed, no further attempt was made to improve this part of the calculated phase diagram. The calculated peritectic temperature of equilibrium $L + \text{Cu}_{51}\text{Zr}_{14} \leftrightarrow \text{Cu}_8\text{Zr}_3$, 1195 K, is much lower than the measured data.^{30,19} The reason for this large difference is that, as discussed in section 3.2, of the two available experimental data, only Kuznetsov et al.¹⁹ was used, and furthermore, a small weight factor was given to it in optimization. The calculated temperature for this equilibrium by Saunders⁵ is in agreement with the result of Lundin et al.³⁰ because they used the data reported by Lundin et al.³⁰ instead of Kuznetsov et al.¹⁹ New experimental work might be needed to study this part of the phase diagram.

The calculated enthalpies of formation of the congruent compounds Cu₅₁Zr₁₄, Cu₁₀Zr₇, and CuZr agree well with the experimental results of Kleppa et al.,¹¹ but that of CuZr₂ is close to the data of Ansara et al.¹² (Table 1). As mentioned in section 3.3, in order to get the eutectoid decomposition of the CuZr phase, its enthalpy of formation must be smaller than the value measured by Ansara et al.¹² Because Saunders did not take into account this eutectoid decomposition and the enthalpy data of the compounds by Kleppa et al.,¹¹ their calculated enthalpy of

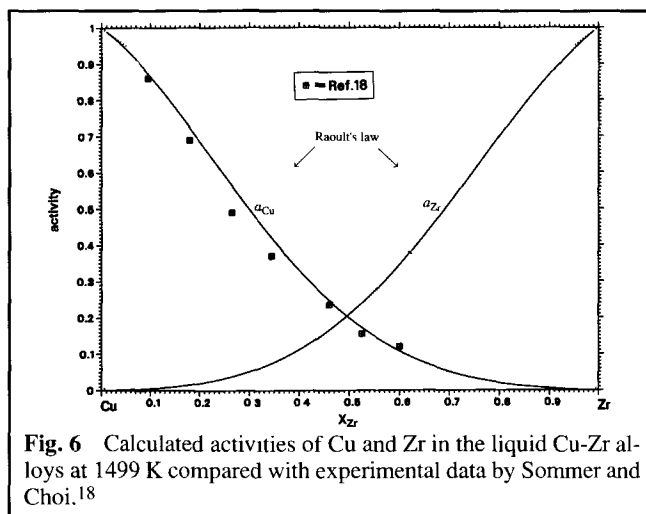


Fig. 6 Calculated activities of Cu and Zr in the liquid Cu-Zr alloys at 1499 K compared with experimental data by Sommer and Choi.¹⁸

CuZr is more negative and, as expected, in good agreement with Ansara et al.¹²

In order to calculate the enthalpies of mixing of the liquid phase $\Delta_{\text{mix}}H^{L-L}$ from the measured heat effects of each addition of zirconium, Kleppa et al.¹¹ took H_{Zr} and $\Delta_{\text{fus}}H_{\text{Zr}}$ from Hultgren et al.,⁵³ but Sommer and Choi¹⁸ took them from Hultgren et al.⁵³ and Guillermet,⁵⁴ respectively. For comparison between these two experimental results and the present calculation, the latest phase stability parameters of H_{Zr} and $\Delta_{\text{fus}}H_{\text{Zr}}$ from Dinsdale¹⁵ were used to recalculate the $\Delta_{\text{mix}}H^{L-L}$ from the reported enthalpies of mixing for Cu(L)₁₃₇₃ + Zr(s)₁₃₇₃ (Ref 11) and Cu(L)₁₄₇₃ + Zr(s)₂₉₈ (Ref 18). Because Sudavtsova et al.¹⁷ did not give the original measured data and the enthalpy data of Zr used in their calculation, their data of $\Delta_{\text{mix}}H^{L-L}$ at 1480 K could not be recalculated here.

Figure 5 compares these recalculated enthalpies of mixing of liquid and the predicted curve. The data of Sommer and Choi¹⁸ were reproduced very well, but those of Sudavtsova et al.¹⁷ seem to be too negative when $x_{\text{Zr}} > 0.2$. The fit to the values of Kleppa et al.¹¹ is not so excellent, but obvious deviations appear only around 16, 32, and 70 at.% Zr, which is similar to the result of Saunders.⁵ The main discrepancy concerns the values at the compositions of 0.1598 and 0.1749 at.% Zr. As these compositions are very close to the liquidus of Cu₅₁Zr₁₄ (the calculated liquidus at 1373 K is about ~17 at.% Zr), it could be reasonably supposed that the measured heat effects for these compositions of samples had included the enthalpy of formation of a small amount of solid phase Cu₅₁Zr₁₄.

Figure 6 shows the variation of calculated a_{Cu} and a_{Zr} with composition in the Cu-Zr liquid alloys at 1499 K. Very good fit has been obtained to the measured a_{Cu} by Sommer and Choi.¹⁸ The activities of both copper and zirconium exhibit a large negative deviation from Raoultian behavior.

The entropy and excess entropy of mixing of liquid Cu-Zr alloys vs compositions calculated using the parameters in Table 7 are given in Fig. 7. Assuming the formation of associates with the stoichiometry Cu₂Zr, Sommer and Choi¹⁸ employed the associate model to describe the thermodynamic properties of liquid Cu-Zr alloys. Their calculated entropy curve and the

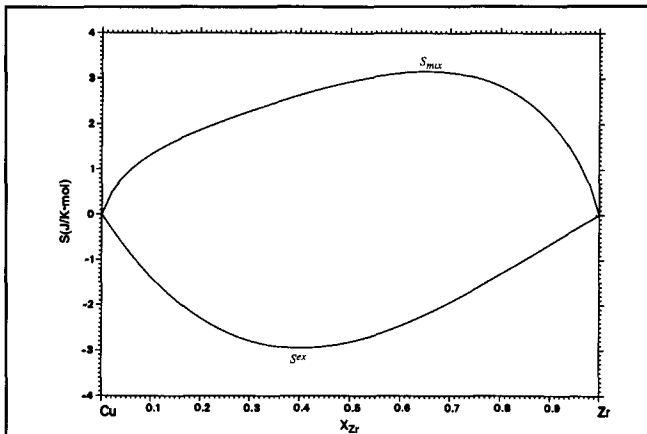


Fig. 7 Calculated entropy and excess entropy of mixing in liquid Cu-Zr alloys vs compositions.

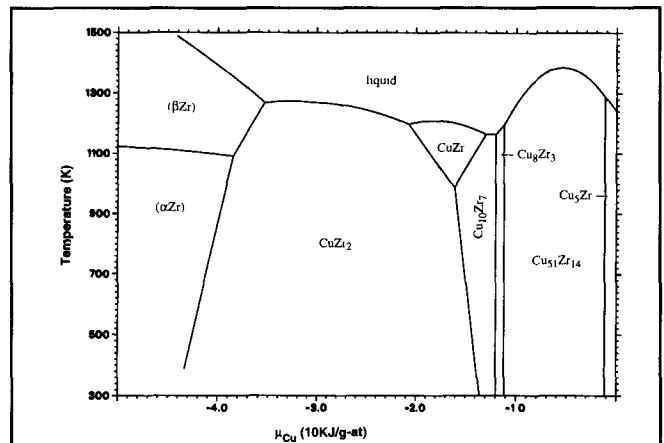


Fig. 8 $\mu_{\text{Cu}}-T$ plots of the Cu-Zr system calculated by using the present thermodynamic description in Table 7.

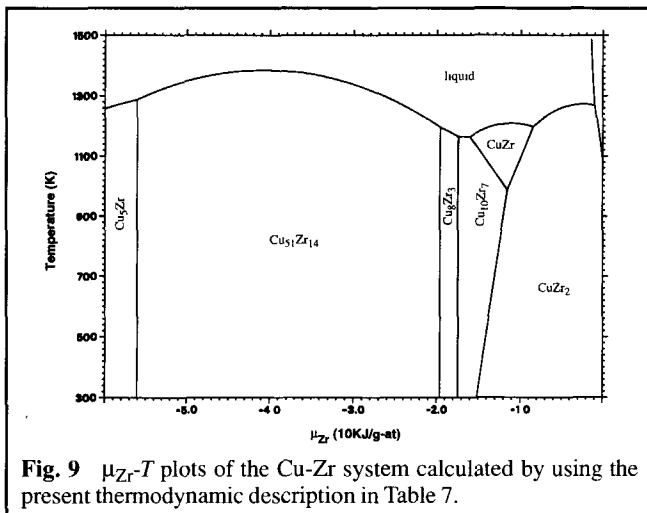


Fig. 9 $\mu_{\text{Zr}}-T$ plots of the Cu-Zr system calculated by using the present thermodynamic description in Table 7.

fit to the enthalpies of mixing of liquid copper with solid zirconium determined by Kleppa et al.¹¹ are very similar to the present calculation shown in Fig. 5 and 7. This means that the tendency of forming associate Cu_2Zr in the liquid alloys is not strong, and the thermodynamic properties of the liquid Cu-Zr alloy can be as well described by the subregular model as the associate model.

Although the predicted thermodynamic properties and the calculated phase diagram of the Cu-Zr system agree very well with the selected experimental data, the reliability of the optimized parameters should be checked further by $\mu-T$ plots of copper and zirconium. In a $\mu-T$ plot, all the two-phase equilibria are represented by lines, which meet at three-phase equilibria represented by points. The areas between the lines represent equilibria of single phases. Lines in this diagram must not cross, except where they end in three-phase equilibria. Otherwise the parts of the lines after the crossing do not represent stable two-phase equilibria. The $\mu_{\text{Cu}}-T$ and $\mu_{\text{Zr}}-T$ plots of the Cu-Zr system calculated using the parameters in Table 7 are presented in Fig. 8 and 9. The reference states for μ_{Cu} and μ_{Zr} are fcc Cu and cph Zr, respectively. These two fig-

ures demonstrate that the estimated H and S values of all the phases in the Cu-Zr system were well chosen.

Acknowledgment

This work was performed at the Laboratory of Materials Processing and Powder Metallurgy, Helsinki University of Technology, Vuorimiehentie, 2K, SF-02150, Espoo, Finland.

The authors are grateful to Professor K. Lilius for providing excellent working conditions at the laboratory. They thank Dr. P. Taskinen for useful advice, and Lic. R. Luoma for his permission to use the experimental data file. One of the authors (K.-J. Z.) wishes to express his special gratitude to Professors Huang Peiyun and Jin Zhanpeng for their constant support, and to thank the Finnish Centre for International Mobility (CIMO) for scholarship. Some of the figures were plotted using Thermo-Calc.

Cited References

1. A.V. Nadkarni and E.P. Weber, *Weld. J.*, 56, 331-338 (1977).
2. V.K. Sarin and N.J. Grant, *Powder Metall. Int.*, 11, 153-157 (1979).
3. *High Conductivity Copper and Aluminum Alloys*, E. Ling and P.W. Taubenblat, Ed., The Metallurgical Society, Warrendale, PA (1984).
4. W.C. Shumay, Jr., *Adv. Mater. Process. inc. Met. Prog.*, 132, 54-60 (1987).
5. N. Saunders, *Calphad*, 9, 297-309 (1985).
6. R. Luoma and J. Talja, Report TTK-V-B61, Helsinki University of Technology, Helsinki, Finland (1991).
7. R. Bormann, F. Gärtner, and F. Haider, *Mater. Sci. Eng.*, 97, 79-81 (1988).
8. M. Hansen and K. Anderko, *Constitution of Binary Alloys*, McGraw-Hill Book Co., New York, 655-657 (1958).
9. R.P. Elliott, *Constitution of Binary Alloys, First Supplement*, McGraw-Hill Book Co., New York, 391 (1965).
10. F.A. Shunk, *Constitution of Binary Alloys, Second Supplement*, McGraw-Hill Book Co., New York, 302-303 (1969).
11. O.J. Kleppa and S. Watanabe, *Metall. Trans. B*, 13, 391-401 (1982).
12. I. Ansara, A. Pasturel, and K.H. Buschow, *Phys. Status Solidi (a)*, 69, 447-453 (1982).
13. T. Massalski, J.L. Murray, L.H. Bennett, and H. Baker, *Binary Alloy Phase Diagrams*, Vol. 1, American Society for Metals, Metals Park, OH, 982 (1986).
14. E. Kneller, Y. Khan, and U. Gorres, *Z. Metallkd.*, 77, 43-48 (1986).

Section I: Basic and Applied Research

15. A.T. Dinsdale, *Calphad*, 15, 317-425 (1991).
16. J.L. Glimois, P. Forey, and J.L. Feron, *J. Less-Common Met.*, 113, 213-224 (1985).
17. S.V. Sudavtsova, G.I. Batalin, A.V. Kalnykov, and F. Kuznetsov, *Sov. Non-Ferrous Met. Res.*, No. 11, 492-493 (1983).
18. F. Sommer and D.K. Choi, *Z. Metallkd.*, 80, 263-269 (1989).
19. G.M. Kuznetsov, V.N. Fedorov, A.L. Rodnyanskaya, and A.V. Nikonova, *Sov. Non-Ferrous Met. Res.*, No. 6, 91-94 (1978).
20. M. Y.-W. Lou and N.J. Grant, *Metall. Trans. A*, 15, 1491-1493 (1984).
21. D. Arias and J.P. Abriata, *Bull. Alloy Phase Diagrams*, 11(5), 452-459 (1990).
22. J.M. Vitek, *Z. Metallkd.*, 67, 559-563 (1976).
23. M.J. Saarivirta, *Trans. Metall. Soc. AIME*, 218, 431-437 (1960).
24. U. Zwicker, *Metall.*, 16, 409-412 (1962).
25. I. Kawakatsu, H. Suzuki, and H. Kitano, *J. Jpn. Inst. Met.*, 31, 1253-1257 (1967).
26. A. Mance and A. Mihajlovic, *J. Appl. Electrochem.*, 11, 299-303 (1981).
27. T.E. Allibone and C. Sykes, *J. Inst. Met.*, 39, 173-189 (1928).
28. S.A. Pogodin, I.S. Shumova, and F.A. Kugucheva, *C. R. Acad. Sci. URSS*, 27, 670-672 (1940).
29. E. Raub and M. Engel, *Z. Metallkd.*, 39, 172-177 (1948).
30. C.E. Lundin, D.J. McPherson, and M. Hansen, *Trans. AIME*, 197, 273-278 (1953).
31. H. Kimura, Y. Minobe, S. Uehara, K. Honma, and N.K. Gakkaishi, *J. Jpn. Inst. Met.*, 37, 552-557 (1973).
32. M.J. Donachie, *J. Inst. Met.*, 92, 180 (1963-1964).
33. P. Forey, J.L. Glimois, and J.L. Feron, *J. Less-Common Met.*, 124, 21-27 (1986).
34. G. von Hillmann and W. Hofmann, *Z. Metallkd.*, 56, 279-286 (1965).
35. L. Meny, M. Champigny, R. Beltrando, and P. Salaun, *J. Microsc.*, 6, 111-112 (1967).
36. A.J. Perry and W. Hugi, *J. Inst. Met.*, 100, 378-380 (1972).
37. V.A. Phillips, *Metallography*, 7, 137-155 (1974).
38. P. Forey, J.L. Glimois, J.L. Feron, G. Devely, and C. Beclé, *C.R. Acad. Sci. (Paris)*, 291, 177-178 (1980).
39. L. Arnborg, U. Backmark, N. Bäckström, and J. Lange, *Mater. Sci. Eng.*, 83, 115-121 (1986).
40. R.P. Singh, A. Lawley, S. Friedman, and Y.V. Murty, *Mater. Sci. Eng. A*, 145, 243-255 (1991).
41. J.P. Gabathuler, P. White, and E. Parthe, *Acta Crystallogr. B*, 31, 608-610 (1975).
42. L. Bsenko, *J. Less-Common Met.*, 40, 365-366 (1975).
43. L. Bsenko, *Acta Crystallogr. B*, 32, 2220-2224 (1976).
44. R.N. Auguston, U.S. Atomic Energy Commission Publ. AECD-3456, Ames Laboratory (1950).
45. W. Showak, *Trans. Metall. Soc. AIME*, 224, 1297-1298 (1962).
46. D.L. Douglass and R.E. Morgan, *Trans. Metall. Soc. AIME*, 215, 869-870 (1959).
47. A.M. Korol'kov and E.V. Lysova, *Strukturai Svoistva Legk. Splavov*, Nauka, Moscow, 17-20 (1971).
48. E.M. Carvalho and I.R. Harris, *J. Mater. Sci.*, 15, 1224-1230 (1980).
49. O. Redlich and A.T. Kister, *Ind. Eng. Chem.*, 40, 345-348 (1948).
50. H.L. Lukas and S.G. Fries, *J. Phase Equilibria*, 13(5), 532-541 (1992).
51. H.L. Lukas, E.-Th. Henig, and B. Zimmermann, *Calphad*, 1, 225-236 (1977).
52. K.H.J. Buschow, *J. Phys. F*, 14, 593 (1984).
53. R. Hultgren, P.D. Desai, D.T. Hawkins, M. Gleiser, K.K. Kelley, and D.D. Wagmann, *Selected Values of the Thermodynamic Properties of the Elements*, American Society for Metals, Metals Park, OH (1973).
54. A.F. Guilletmet, *High Temp.-High Press.*, 19, 119-160 (1987).
55. R.P. Singh and A. Lawley, *Metall. Trans. A*, 23, 3393-3394 (1992).